

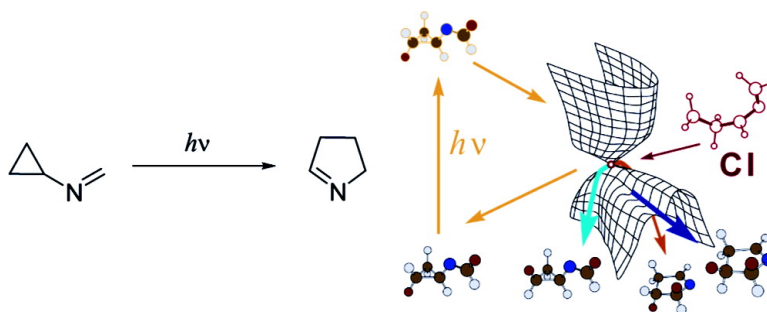
Article

Mechanism of the *N*-Cyclopropylimine-1-pyrroline Photorearrangement

Diego Sampedro, Alberto Soldevilla, Miguel A. Rodriguez, Pedro J. Campos, and Massimo Olivucci

J. Am. Chem. Soc., **2005**, 127 (1), 441-448 • DOI: 10.1021/ja0467566 • Publication Date (Web): 04 December 2004

Downloaded from <http://pubs.acs.org> on March 24, 2009



More About This Article

Additional resources and features associated with this article are available within the HTML version:

- Supporting Information
- Links to the 2 articles that cite this article, as of the time of this article download
- Access to high resolution figures
- Links to articles and content related to this article
- Copyright permission to reproduce figures and/or text from this article

[View the Full Text HTML](#)

Mechanism of the *N*-Cyclopropylimine-1-pyrroline Photorearrangement

Diego Sampedro,^{*,†} Alberto Soldevilla,[†] Miguel A. Rodríguez,[†]
Pedro J. Campos,[†] and Massimo Olivucci[‡]

Contribution from the Departamento de Química, Universidad de La Rioja, Grupo de Síntesis Química de La Rioja, Unidad Asociada al C.S.I.C., Madre de Dios, 51, E-26006 Logroño, Spain, and Dipartimento di Chimica, Università degli studi di Siena, Via Aldo Moro 2, I-53100 Siena, Italy

Received June 2, 2004; E-mail: diego.sampedro@dq.unirioja.es

Abstract: We present here a combined experimental and computational investigation into the photorearrangement of *N*-cyclopropylimines to yield pyrrolines. We show that the photochemistry, regiochemistry, and stereochemistry of the reaction can be understood in terms of a mechanism involving barrierless evolution in three different (S_2 , S_1 , S_0) singlet states and sequential decay through two different (S_2/S_1 , and S_1/S_0) conical intersection funnels. We provide evidence that the reaction mechanism involves the generation of a nonequilibrated (i.e., transient) excited state diradical, whose decay can lead not only to pyrrolines but also to cyclopropylimine isomers. It is concluded that the reaction outcome depends on the details of the structure of such transient diradical and on the nature of the dynamics of its decay through the S_1/S_0 conical intersection.

1. Introduction

In 1959, Neureiter reported the first example of a vinylcyclopropane–cyclopentene-type thermal rearrangement.¹ Ten years later, Woodward and Hoffmann used this rearrangement as an example of a [1,3] sigmatropic reaction.² The publication of this paper greatly contributed to an increase in the interest in this reaction.^{3–7} Since then, the study of the simplest known [1,3] sigmatropic shift has attracted the attention of both experimentalists and computational chemists: reaction kinetics,⁸ substituent effects,^{9,10} reaction stereochemistry,^{11–14} and theoretical calculations^{15–17} have been the subject of numerous

investigations and are still topics of current research.^{14b} As a consequence, the vinylcyclopropane to cyclopentene rearrangement is now a useful tool for retrosynthetic analyses.¹⁸

In contrast with the widely studied thermal reaction, the photochemical version of the [1,3] sigmatropic shift has been explored to a much lesser extent. However, the photochemical rearrangements of vinylcyclopropanes have been reported under both direct and sensitized conditions.^{19–21} Although these transformations are of mechanistic interest, practical applications are scarce and most of them deal with strained bicyclic compounds.²² As a modification of the basic reaction, we recently reported the photochemical rearrangement of *N*-cyclopropylimines to 1-pyrrolines.²³ Unlike its all-C analogue, the photoreaction of the *N*-substituted vinylcyclopropanes proceeds in a synthetically useful way since the final 1-pyrrolines can often be isolated in good yields. The corresponding thermal rearrangement has also been reported.^{24,25}

Vinylcyclopropane rearrangements and related reactions have also been the subject of theoretical studies. However, initial attempts did not give good results because of computational limitations. Only in the past decade have computational tools provided interesting results regarding the thermal rearrangement

[†] Universidad de La Rioja.

[‡] Università degli studi di Siena.

- (1) Neureiter, N. P. *J. Org. Chem.* **1959**, *24*, 2044.
- (2) Woodward, R. B.; Hoffmann, R. *Angew. Chem., Int. Ed. Engl.* **1969**, *8*, 781.
- (3) Hudlický, T.; Kutchan, T. M.; Naqvi, S. M. *Org. React.* **1985**, *33*, 247.
- (4) Baldwin, J. E. *J. Comput. Chem.* **1988**, *19*, 222.
- (5) Wong, H. N. C.; Hon, M.-Y.; Tse, C.-W.; Yip, Y.-C.; Tanko, J.; Hudlický, T. *Chem. Rev.* **1989**, *89*, 165.
- (6) Hudlický, T.; Reed, J. W. In *Comprehensive Organic Chemistry*; Trost, B. M., Fleming, I., Eds.; Pergamon: Oxford, 1991; Vol. 5, p 899.
- (7) Baldwin, J. E. *Chem. Rev.* **2003**, *103*, 1197.
- (8) De Wolfe, R. H. In *Comprehensive Chemical Kinetics*; Bamford, C. H., Tipper, C. F. H., Eds.; Elsevier: New York, 1973; Vol. 9, p 417.
- (9) Simpson, J. M.; Richey, H. G. *Tetrahedron Lett.* **1973**, 2545.
- (10) McGaffin, G.; Grimm, B.; Heinecke, U.; Michaelsen, H.; de Meijere, A.; Walsh, R. *Eur. J. Org. Chem.* **2001**, 3559.
- (11) Andrews, G. D.; Baldwin, J. E. *J. Am. Chem. Soc.* **1975**, *97*, 5512.
- (12) Newman-Evans, R. H.; Simon, R. J.; Carpenter, B. K. *J. Org. Chem.* **1990**, *55*, 695.
- (13) Asuncion, L. A.; Baldwin, J. E. *J. Am. Chem. Soc.* **1995**, *117*, 10672.
- (14) (a) Olson, L. P.; Niwayama, S.; Yoo, H.-Y.; Houk, K. N.; Harris, N. J.; Gajewski, J. J. *J. Am. Chem. Soc.* **1996**, *118*, 886. (b) Doering, W. E.; Barsa, E. A. *J. Am. Chem. Soc.* **2004**, *126*, 12353.
- (15) Davidson, E. R.; Gajewski, J. J. *J. Am. Chem. Soc.* **1997**, *119*, 10543.
- (16) Houk, K. N.; Nendel, M.; Wiest, O.; Storer, J. W. *J. Am. Chem. Soc.* **1997**, *119*, 10545.
- (17) Doubleday, C. J. *Phys. Chem. A* **2001**, *105*, 6333.

- (18) Corey, E. J.; Cheng, X.-M. *The Logic of Chemical Synthesis*; J. Wiley: New York, 1989; p 88.
- (19) Jorgenson, M. J. *J. Am. Chem. Soc.* **1966**, *88*, 3463.
- (20) Zimmerman, H. E.; Epling, G. A. *J. Am. Chem. Soc.* **1972**, *94*, 8638.
- (21) Hahn, R. C.; Johnson, R. P. *J. Am. Chem. Soc.* **1976**, *98*, 2600.
- (22) Sonawane, H. R.; Bellur, N. S.; Kulkarni, D. G.; Ahuja, J. R. *Synlett* **1993**, *12*, 875.
- (23) Campos, P. J.; Soldevilla, A.; Sampedro, D.; Rodríguez, M. A. *Org. Lett.* **2001**, *3*, 4087.
- (24) Caramella, P.; Huisgen, R.; Schmolke, B. *J. Am. Chem. Soc.* **1974**, *96*, 2997.
- (25) Campos, P. J.; Soldevilla, A.; Sampedro, D.; Rodríguez, M. A. *Tetrahedron Lett.* **2002**, *43*, 8811.

Table 1. Rearrangement of *N*-Cyclopropylimines To Give Pyrrolines (**1a–j** → **2a–j**)^e

<i>N</i> -cyclopropylimine	R ¹	R ²	R ³	R ⁴	t (h)	yield (%)
1a	H	H	H	Ph	6	70
1b	H	H	Me	Ph	6	65
1c	H	H	Ph	Ph	5	80
1d	H	Ph	H	Ph	5	65 ^{a,b}
1e	H	Ph	Me	Ph	5	60 ^{a,c}
1f	H	Ph	Ph	Ph	4	85 ^a
1g	Ph	H	H	Ph	0.75	70
1h	H	OBu	H	Ph	3	45 ^d
1i	Ph	H	Ph	Ph	0.5	80
1j	Ph	H	H	<i>trans</i> -CH=CHPh	5	50 ^a

^a Pyrex filtered. ^b Pyrroline was oxidized to pyrrole during the workup. ^c Mixture of two stereoisomers. ^d Only the *trans* isomer could be isolated. ^e See also Scheme 1.

and its stereochemistry. CASSCF and DFT calculations were used to calculate the *si* path (see below).^{15,16} More recently, trajectory studies have been used to predict product distributions.¹⁷ However, to the best of our knowledge, theoretical studies dealing with the photochemical version of these reactions have not been published.

To achieve a deeper knowledge of the *N*-cyclopropylimine rearrangement, we present here a thorough study of the mechanism of its photochemical transformation to pyrrolines. Accordingly, in Section 2 we present the results of product and stereochemical analysis of the reaction, and in Section 3 we describe the result of complementary state-of-the-art ab initio quantum chemical calculations that establish the general reaction mechanism.

2. Experimental Results

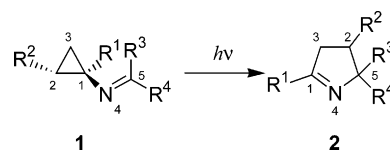
2.1. Synthesis and Photorearrangement. Several methods for the preparation of cyclopropylamines have been reported to date.^{26,27} Condensation of amines and different carbonyl compounds²³ yielded a set of *N*-cyclopropylimines with different substitution patterns. Groups such as H, alkyl, and aryl, as well as electron-donating groups, can easily be introduced at any site of the cyclopropylimine moiety. For electron-withdrawing groups in C-2, this methodology cannot be directly applied because of the tendency of the corresponding cyclopropylamines to open spontaneously under the reaction conditions.^{28,29} This limitation can be overcome using an approach based on a one-pot two-step process involving irradiation of Fischer imine-carbene complexes in the presence of alkenes substituted with electron-withdrawing groups.³⁰ In these reactions, the *N*-cyclopropylimines (which subsequently rearrange to yield pyrrolines) are formed in situ by a cycloaddition process.

Irradiation of the *N*-cyclopropylimines prepared with a medium-pressure 400-W mercury lamp afforded the corresponding pyrrolines in good yields. Table 1 shows the results obtained. Remarkably, the reaction allows the use of substituents that differ in size and nature and are located in different positions on both the cyclopropane and imine moieties without a significant influence on the product yield.

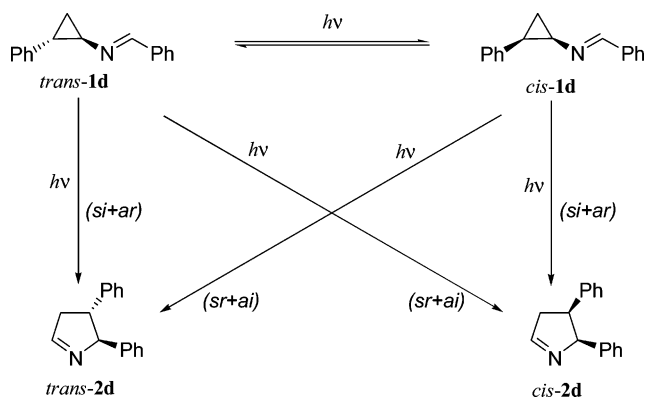
The mechanistic studies presented below are limited to cyclopropylimine **1d** (see Scheme 2), **1e**, and **1f** as their stereochemical outcome can be easily determined by NMR. The main transformations to be considered are shown in Scheme 2.

From *trans*-**1d**, three different compounds can be formed through different reaction paths. Besides the formation of two different

Scheme 1



Scheme 2



diastereomeric pyrrolines (*trans*- and *cis*-**2d**), the cyclopropylimine can also undergo ring isomerization to give the cyclopropylimine *cis*-**1d**, which can, in turn, rearrange to the same two pyrrolines, *trans*- and *cis*-**2d** (throughout the paper *trans*- and *cis*- refer to the ring stereochemistry and not to the stereochemistry of the imine double bond). As shown in Scheme 2, the rearrangement from cyclopropylimines to pyrrolines can occur through two stereochemically different paths, which are denoted using the Woodward–Hoffmann² notation. Accordingly, *s* and *a* (suprafacial, antarafacial) and *r* and *i* (retention, inversion) refer to the stereochemical outcomes for the 1, 3-shift process involved. We found that, in contrast to cyclopropylamines, the different pyrrolines remain stable, both thermally and photochemically.³¹

To exclude the possible influence of the solvent on the rearrangement mechanism or the product distribution, we carried out the irradiation of *trans*-**1d** in a variety of solvents of different polarity (e.g., hexane, THF, CH₂Cl₂, benzene, acetonitrile, DMSO) and monitored both the rearrangement and ring isomerization. The lack of influence of the solvent polarity on the rearrangement suggests that a charged intermediate is not involved in the reaction mechanism. However, the solvent appears to influence the extent of the undesirable polymerization, indirectly affecting the reaction yield. This is especially noticeable in the cyclopropylaldimines, because of the less steric hindrance of the iminic carbon. Consistently, any correlation between the experimental parameters for the solvents and the reaction yields could not be found for the thermal version of the rearrangement.²⁴ However, some correlation between the extent of polymerization and the Taft scale of polarities was observed, with the more polar solvents giving cleaner reactions.

2.2. Stereochemistry. A range of different cyclopropylimines was investigated to determine their reactivities and to study the associated regiochemistry and stereochemistry. For substituted cyclopropanes with R² ≠ H (e.g., **1d–1f** in Table 1), two different regioisomers of the pyrroline products could, in principle, be formed depending on the cyclopropane bond that breaks during the rearrangement. However, in a manner consistent with the situation shown in Scheme 1, in all cases considered only one of the cyclopropane bonds took part in the rearrangement, meaning that the reaction is highly regioselective. The same trend has been observed for the thermal vinylcyclopropane–cyclopentene rearrangement,⁷ where the observed regioisomer is related to the ability of the different groups to stabilize the radical formed

(26) Vilsmaier, E. In *The Chemistry of the Cyclopropyl Group*; Rappoport, Z., Ed.; Wiley: New York, 1987; pp 1341–1454.

(27) Bertus, P.; Szymoniak, J. *J. Org. Chem.* **2003**, *7133*.

(28) Reissig, H. U. *Top. Curr. Chem.* **1988**, *144*, 73.

(29) Magenlinckx, S.; De Kimpe, N. *Tetrahedron Lett.* **2003**, *44*, 1771.

(30) Campos, P. J.; Sampedro, D.; Rodríguez, M. A. *Organometallics* **2002**, *21*, 4076.

(31) We have checked the thermal and photochemical stability of pyrrolines by heating pure samples in refluxing toluene and irradiating them under the same reaction conditions. In both cases, we recovered the unaltered products after 5 h.

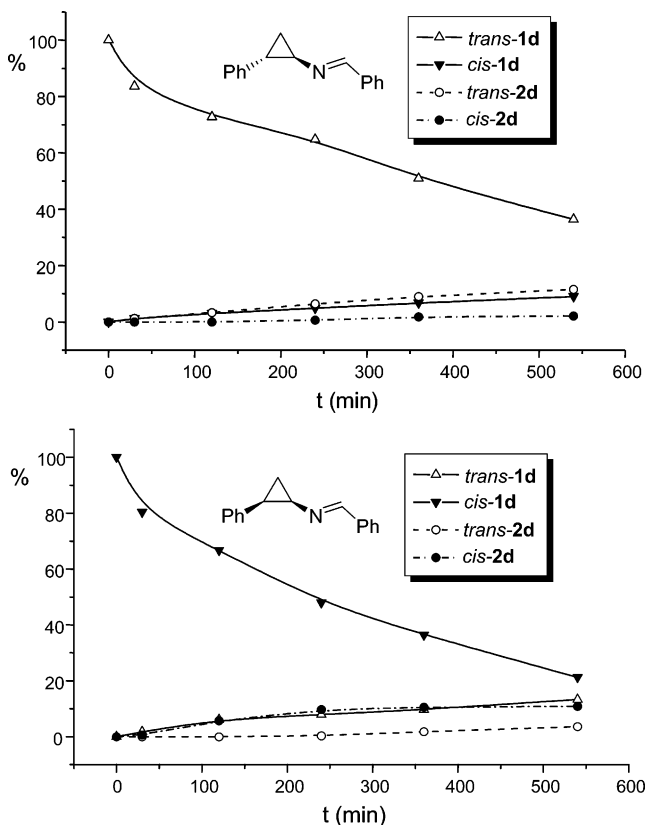


Figure 1. Evolution of the reaction mixture composition during irradiation of **1d**.

during the reaction. In contrast to the well-understood regiochemistry, the stereochemistry of these rearrangements has been the subject of much research in recent decades.^{11–14} The main difficulty is to obtain information on the stereochemistry in the presence of competing reactions such as racemization or ring isomerization, both of which cause stereochemical scrambling.

To investigate the influence of the substitution at the C₂ carbon of the cyclopropyl ring on the reaction stereochemistry, we have studied the photorearrangement of *cis*- and *trans*-**1d** independently. In the experiment, we employed ¹H NMR to monitor the progress of both ring isomerization and rearrangement of *cis* and *trans*-**1d** (see Supporting Information for details). The results displayed in Figure 1 show that the two reactions occur with roughly the same rate constant. On the other hand, there is a clear preference for the formation of the *cis*-**2d** pyrroline when the starting imine is *cis*-**1d**. Similarly, we found that *trans*-**1d** preferentially produces the *trans*-**2d** pyrroline. For short irradiation times (less than 240 min), this preference is high (the ratio is more than 10:1 for the formation of the preferred pyrroline). However, the stereoselectivity decreases for longer irradiation times. When the reaction is completed, the observed ratio is 5:1. In fact, irrespective of the initial stereochemistry of the reactant (i.e., *cis* or *trans*), both pyrroline stereoisomers are detected. Long irradiation times (more than 240 min) also lead to ring isomerization in both samples in the same ratio. More specifically, we detected the formation of a mixture of cyclopropanes with *cis*/*trans* ratios of 0.9:1 that must be determined by their relative UV absorbance and isomerization quantum yields. The loss of material observed after irradiation is due to production of a polymer. Such atactic polymer could be isolated and weighed to ensure the mass balance, but it was not further studied.

The effect of the substitution at the iminic carbon was assessed by monitoring the photorearrangement of *trans*-**1e** where a hydrogen atom is replaced by a methyl (i.e., R³ = CH₃). The results are shown in Figure 2. The formation of both *trans*- and *cis*-**2e** occurs from the very beginning with an approximate product ratio of 3:1, which is clearly

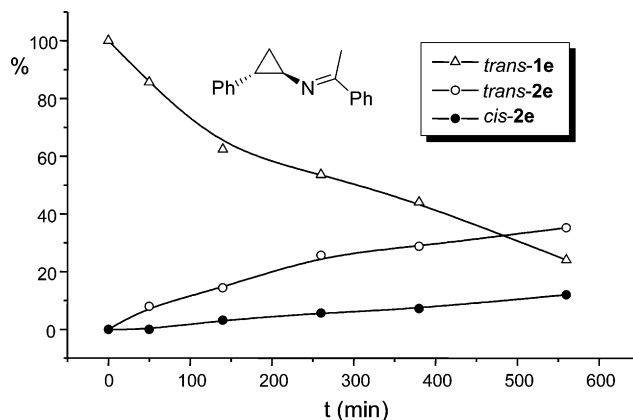


Figure 2. Evolution of the reaction mixture composition during irradiation of *trans*-**1e**.

lower than the 5:1 ratio detected for the reference compounds *trans*- and *cis*-**1d**. This behavior shows that the substituent does affect the diastereoselectivity of the rearrangement.

In the final step of our stereochemical studies, we investigated the rearrangement of two enantiopure compounds. This study provided mechanistic information about the relative ratio of racemization compared with the competing ring isomerization and rearrangement. Furthermore, this investigation also provided a gage of the potential synthesis of enantiopure pyrrolines. The (–)-(1*R*,2*S*) and (+)-(1*S*,2*R*) enantiomers of cyclopropylimine **1f** were synthesized and irradiated. We determined the enantiomeric purity of the resulting mixture (see Supporting Information). The results show that, even after short reaction times, the rate of racemization of the starting material is faster than the structural isomerization to pyrroline products. Racemization could potentially occur through two consecutive processes of ring breaking—single bond rotation (to yield a *cis* diastereoisomer, i.e., 1*R*,2*R* or 1*S*,2*S*, in the first step and a *trans* enantiomer in the second step) involving a diradical intermediate or through a Doering's path involving a non-equilibrated diradical species.³²

2.3. Photochemical Aspects. As mentioned above, the cyclopropylimine photorearrangement has a thermal equivalent.²⁵ Thus, to ensure that the investigated rearrangement is photochemically (i.e., not thermally) induced, we tested the thermal stability of the reactants. Several imines (**1a**, **1b**, *t*-**1e**, *t*-**1f**, **1h**) were heated under reflux in toluene for 3 days and no traces of the corresponding pyrrolines were detected. Indeed, the thermal rearrangement requires a temperature of ca. 350 °C under flash vacuum pyrolysis conditions.²³

Figure 3 shows the UVA absorption spectra for three compounds with different substitution patterns. It can be seen from this figure that all spectra have the same basic structure, with a strong absorption responsible for the reaction at ca. 250 nm. An additional band at higher energy and of variable strength can also be seen if aromatic substituents are present. The cyclopropane moiety has been described to act as a modest auxochrome, causing small displacements of ca. 10–20 nm in the absorption bands of the olefins.³³ This behavior was detected in derivatives with a phenyl group on C₂ (e.g., for compound *trans*-**1e**). It can be concluded that efficient interaction between the cyclopropane and phenyl rings can only be achieved when the aromatic ring is located in position 2. A practical consequence of this situation is that 2-phenyl-substituted cyclopropylimines present a significant absorption over 300 nm and, therefore, they can be irradiated through a Pyrex filter. The nature of the excited-state involved in the rearrangement was investigated by carrying out the reaction in the presence of molecular oxygen or *Z*-piperlyene as triplet state quenchers. No influence beyond experimental error could be detected in these experiments, indicating that the excited state responsible for the rearrangement should have a

(32) Doering, W. E.; Sachdev, K. *J. Am. Chem. Soc.* **1974**, *96*, 1168.

(33) Goldschmidt, Z.; Crammer, B. *Chem. Soc. Rev.* **1988**, *17*, 229.

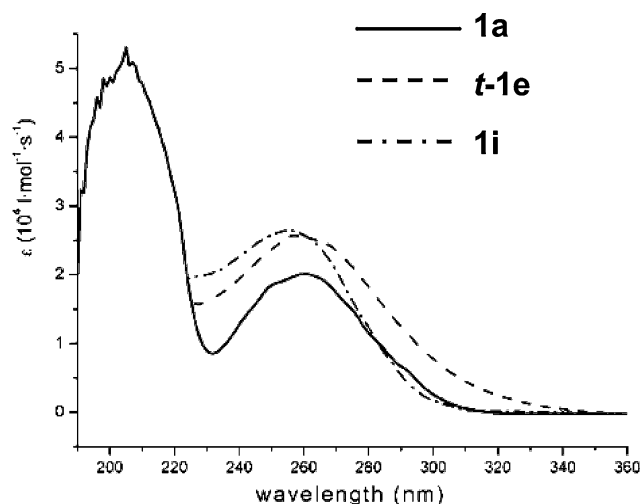


Figure 3. UVA absorption spectra for some representative *N*-cyclopropylimines.

singlet multiplicity. Finally, the fact that we were unable to detect any measurable fluorescence from the photoexcited cyclopropylimines suggests the presence of a readily accessible radiationless deactivation path.

The photorearrangement and photoisomerization quantum yields were determined for **1d** by using ferrioxalate as an actinometer³⁴ (for details see Supporting Information). The measured quantum yield for the rearrangement was extrapolated to zero conversion and gave a value of $\Phi = 0.002(2)$. Similarly, the corresponding quantum yield for the ring isomerization is $\Phi = 0.002(3)$ for both the cis-to-trans and trans-to-cis conversions. These values demonstrate the photochemical inefficiency of the reactions. However, since the pyrroline products are stable under the reaction conditions (see discussion above) and no other compounds are formed during the reaction, these products can still be obtained in good yields through prolonged irradiation. The deactivation of the excited state of cyclopropylimines through a *Z/E* isomerization of the double bond is a well-known feature of imines.³⁵

The quantum yield of the ring isomerization was sensitive to the substituents on the iminic carbon. For example, when we measured the quantum yield for the isomerization of **1f**, which has two phenyl groups on the iminic carbon, we found a quantum yield for the cis-to-trans ring isomerization of $\Phi = 0.005(7)$, while the value for the rearrangement quantum yield was $\Phi = 0.002(5)$. Direct comparison of imines **1d** and **1f** shows similar quantum yields for the rearrangement but a higher cis-to-trans isomerization quantum yield for compound **1f**. It appears that the higher steric demand on the iminic carbon leads to more effective cis-to-trans isomerization while making the reverse trans-to-cis reaction more difficult. This fact could be related to the absence of ring isomerization seen in Figure 2 for *trans*-**1e**, where no significant amount of *cis*-**1e** was detected throughout the experiment, probably because of its faster reaction rate.

3. Theoretical Results.

3.1. Computational Details. All reaction paths were computed using fully unconstrained ab initio quantum chemical computations in the framework of a CASPT2//CASSCF^{36,37} strategy. This requires the reaction coordinate to be computed at the complete active space self-consistent field (CASSCF) level of theory and the corresponding energy profile to be reevaluated

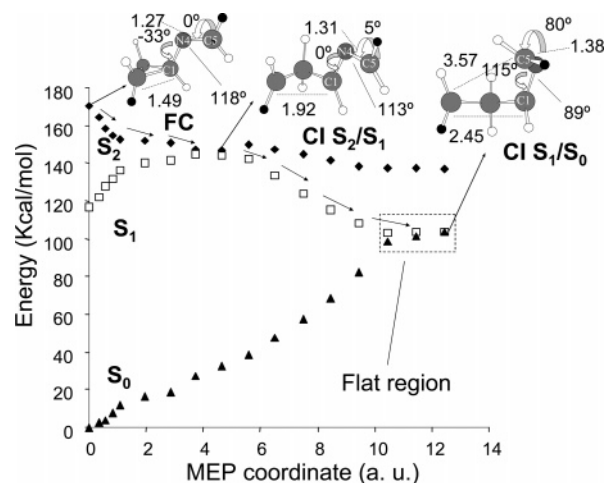


Figure 4. Energy profiles along the MEPs describing the excited-state relaxation from the FC point (Franck–Condon, vertical excitation) of model compound **3**. Geometrical parameters are shown in Å and degrees. The dashed frame highlights the flat region near the CI point (conical intersection).

at the multiconfigurational second-order Møller–Plesset perturbation theory level (here we used the CASPT2 method implemented in MOLCAS-5)³⁸ to take into account the effect of electron dynamic correlation. The calculation of the reaction path (see Figure 4) was performed using the simple *N*-cyclopropylimine **3**, whereas the reaction stereochemistry was computationally investigated using the methyl-substituted derivative **4**. Similarly, the effect of the position and nature of the substituent was determined on the phenyl-substituted models **1a**, **5**, **6**, and **7**. Finally, the effect of the cis–trans ring isomerization mechanism was further investigated on derivatives **8** and **9**. All branches of the reaction coordinate for **3** and **4** were obtained by minimum energy path (MEP) computations at the CASSCF level with the 6-31G* basis set and an active space of six electrons in five orbitals (π and π^* orbitals of the imine moiety, σ and σ^* orbitals for the C₁–C₂ bond, and the nitrogen atom n orbital). The zeroth order wave function used in the single-point CASPT2 calculations needed for the re-evaluation of the MEP energy profile (see above) is a three root (S_0 , S_1 , S_2) state average CASSCF wave function. The same type of wave function was used, where necessary, to avoid convergence problems. The structure of the conical intersection funnels associated with each path were optimized by applying the methodology included in GAUSSIAN 98.³⁹ In all cases, the S_0 branches of the different paths (i.e., the S_0 relaxation paths) starting at the S_1/S_0 conical intersection funnels and describing

(38) Andersson, K.; Barisz, M.; Bernhardsson, A.; Blomberg, M. R. A.; Cooper, D. L.; Fleig, T.; Fülscher, M. P.; de Graaf, C.; Hess, B. A.; Karlström, G.; Lindh, R.; Malmqvist, P.-Å.; Neogrády, P.; Olsen, J.; Roos, B. O.; Schmelpfennid, B.; Schültz, M.; Sadlej, A. J.; Schütz, M.; Seijo, L.; Serrano-Andrés, L.; Siegbahn, P. E. M.; Stårling, J.; Thorsteinsson, T.; Veryazov, V.; Widmark, P.-O.; MOLCAS: version 5.1; University of Lund, Sweden, 2000.

(39) Frisch, M. J.; Trucks, G. W.; Schlegel, H. B.; Scuseria, G. E.; Robb, M. A.; Cheeseman, J. R.; Zakrzewski, V. G.; Montgomery, J. A., Jr.; Stratmann, R. E.; Burant, J. C.; Dapprich, S.; Millam, J. M.; Daniels, A. D.; Kudin, K. N.; Strain, M. C.; Farkas, O.; Tomasi, J.; Barone, V.; Cossi, M.; Cammi, R.; Mennucci, B.; Pomelli, C.; Adamo, C.; Clifford, S.; Ochterski, J.; Petersson, G. A.; Ayala, P. Y.; Cui, Q.; Morokuma, K.; Malick, D. K.; Rabuck, A. D.; Raghavachari, K.; Foresman, J. B.; Cioslowski, J.; Ortiz, J. V.; Baboul, A. G.; Stefanov, B. B.; Liu, G.; Liashenko, A.; Piskorz, P.; Komaromi, I.; Gomperts, R.; Martin, R. L.; Fox, D. J.; Keith, T.; Al-Laham, M. A.; Peng, C. Y.; Nanayakkara, A.; Gonzalez, C.; Challacombe, M.; Gill, P. M. W.; Johnson, B.; Chen, W.; Wong, M. W.; Andres, J. L.; Gonzalez, C.; Head-Gordon, M.; Replogle, E. S.; Pople, J. A. *Gaussian 98*, Revision A.7; Gaussian Inc.: Pittsburgh, PA, 1998.

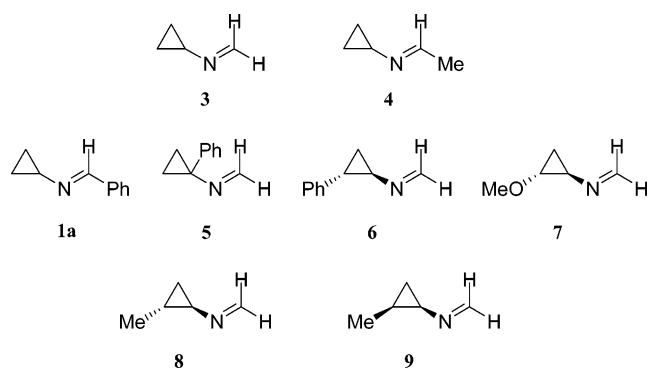
(34) Murov, S. L.; Carmichael, I.; Hug, G. L. *Handbook of Photochemistry*, 2nd ed.; Marcel Dekker: New York, 1993; p 299.

(35) Klessinger, M.; Michl, J. *Excited States and Photochemistry of Organic Molecules*; VCH: New York, 1995.

(36) Ferre, N.; Olivucci, M. *J. Am. Chem. Soc.* **2003**, *125*, 6868.

(37) González-Luque, R.; Garavelli, M.; Bernardi, F.; Merchán, M.; Robb, M. A.; Olivucci, M. *Proc. Natl. Acad. Sci. U.S.A.* **2000**, *97*, 9379.

Scheme 3



the formation of the photoproducts (and the reconstitution of the original reactant) were computed according to the procedure previously described.⁴⁰ To explore the substitution effect in **5–6**, we used a complete active space of 12 electrons in 11 orbitals with the 6-31G* basis set, followed by three root (S_0 , S_1 , S_2) CASPT2 calculations.

3.2. Absorption Spectra. We calculated the absorption spectra for several *N*-cyclopropylimines with different substitution patterns (see Scheme 3). Compound **1a** allows for a comparison of theoretical and experimental data. The calculated $n-\pi^*$ $S_0 \rightarrow S_1$ transition presents an oscillator strength of 0.003, with a λ_{\max} of 297 nm, while the $\pi-\pi^*$ $S_0 \rightarrow S_2$ transition has an oscillator strength of 0.38 with a $\lambda_{\max} = 227$ nm (126 kcal/mol). These values are consistent with the experimental spectrum in Figure 3, where the band appears at 210 nm (136 kcal/mol) with $f = 0.31$. Despite the lack of experimental data, we also calculated the UV spectra for compounds **5–7** to assess the influence of the substituent position and type. For these species, we found the same two bands at similar wavelengths and with S_2 playing the role of the spectroscopic state.

3.3. Compound 3. The calculated S_2 MEP is shown in Figure 4. In the vertical excitation region, S_2 features a charge-transfer character as, upon photoexcitation, an electron is shifted from the imine moiety to the cyclopropane ring. Along the S_2 relaxation path the cyclopropane ring, which now has a radical anion character, spontaneously opens because of the coupling between the imine π and the ring σ^* orbitals—a process that increases the occupancy of the σ^* orbital. Indeed, the first part of the MEP coordinate is controlled by C–C bond elongation, which leads to stabilization of the S_2 state and, as a consequence, to a decrease in the S_2-S_1 energy gap. This process ultimately leads to a conical intersection point (CI_{S_2/S_1}) that provides a fully efficient relaxation channel to the lower $n-\pi^*$ energy surface. After the decay, the S_1 reaction coordinate becomes dominated by twisting along the N_4-C_5 bond as this bond has now completely lost its double-bond character. More specifically, the torsional deformation is mainly driven by the stabilization of the radical center located on the iminic part and this is achieved by combined rotation along the N_4-C_5 and C_1-N_4 bonds. This relaxation does not lead to any energy minima (i.e., to production of an excited-state intermediate) but provides direct access to a second conical intersection decay channel connecting the S_1 and S_0 energy surfaces. At this stage, the details of the geometrical structure of the molecule (which has

now a diradical character) and the structure of the emerging S_0 relaxation paths will affect the product distribution. In particular, the S_1/S_0 conical intersection (CI_{S_1/S_0}) structure features a ca. 90° twisted methylene group at C5. Since rotation about the N_4-C_5 bond can occur in both the clockwise and counterclockwise directions, the decay at CI_{S_1/S_0} will strongly affect the rearrangement reaction suprafacial/antarafacial stereochemistry of the reaction. In **3**, the two iminic substituents are the same ($R^3 = R^4 = H$) and thus the clockwise and counterclockwise rotations will lead to the same structure (see Section 3.4 for a case where these motions lead to different structures). However, one can still compute two stereochemically different relaxation paths associated with the supra or antarafacial processes, respectively. Since the iminic substituents in **3** are both hydrogen atoms, the two paths are almost isoenergetic. For this reason only, one of these paths (clockwise) is shown in Figure 4. Regrettably, however, the shape of the S_1 potential energy surface in the vicinity of the decay region is always very flat (see dashed frame in Figure 4) and it is not possible to assign a specific stereochemical motion to the excited state. (The flatness of the PES in S_0 has previously been described for related reactions.^{15,16}) This region of the S_1 surface is described by a nonequilibrium open chain diradical species (where the diradical centers are located on C5 and C2) whose structure is related to that of the conical intersection CI_{S_1/S_0} (see Figure 4). This structure is strongly reminiscent of the so-called continuous diradical proposed by Doering et al. for explaining the stereochemical behavior associated with thermal cyclopropane ring openings.³² According to Doering, since these diradicals are not equilibrated (i.e., they do not correspond to a well-defined energy minimum), they mediate so-called direct reactions. From a dynamical point of view, the behavior as a continuous diradical will depend on the S_1/S_0 crossing efficiency. If the S_1/S_0 crossing efficiency is high (leading to an S_1 lifetime time well under 1 ps), then products are formed rapidly and S_1 behaves like a continuous diradical. The fact that we find no transition structure (i.e., no energy barrier) along the computed MEP restraining decay at CI_{S_1/S_0} and that the flat region of the S_1 energy surface is nearly degenerate (see framed region in Figure 4) strongly support such assignment. We will now see that the almost free rotation about the N_4-C_5 and C_1-N_4 single bonds allows for the presence of different, almost isoenergetic, reaction paths preparing the system to decay toward the different experimentally detected products. In such a situation, both structural and dynamic factors must contribute to determine the reaction stereochemistry, and therefore the behavior of the system in this region has to be investigated using nonadiabatic dynamics (either in its semiclassical or quantum formulation). This type of investigation goes beyond the scope of the present paper.

Once the molecule reaches the CI_{S_1/S_0} region, decay to the ground state is fully efficient. Figure 5 shows the branching space at CI_{S_1/S_0} that comprises two independent directions of nuclear motion (\mathbf{x}_1 and \mathbf{x}_2). Any molecular motion with a component along one of these directions takes the system away from the S_1/S_0 degeneracy and, thus, initiates the relaxation along the S_0 energy surface.

Motion along the direction described by \mathbf{x}_1 affords the formation of the pyrroline from the CI_{S_1/S_0} region while \mathbf{x}_2 describes cyclopropylimine back formation. On the other hand, movement along the \mathbf{x}_1 or \mathbf{x}_2 directions causes the formation of

(40) Garavelli, M.; Celani, P.; Fato, M.; Bearpark, M. J.; Smith, B. R.; Olivucci, M.; Robb, M. A. *J. Phys. Chem. A* **1997**, *101*, 2023.

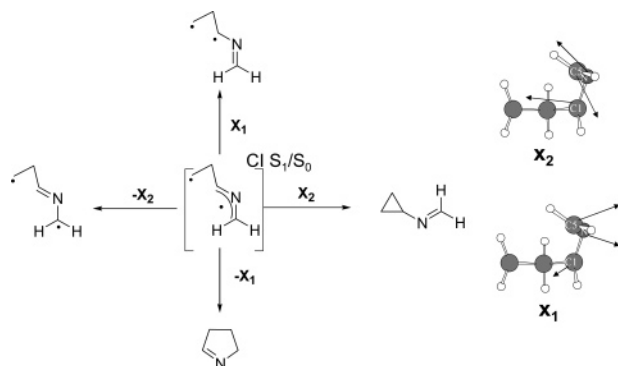


Figure 5. Gradient difference vector \mathbf{x}_1 and derivative coupling vector \mathbf{x}_2 computed at CI_{S_1/S_0} for model compound **3**.

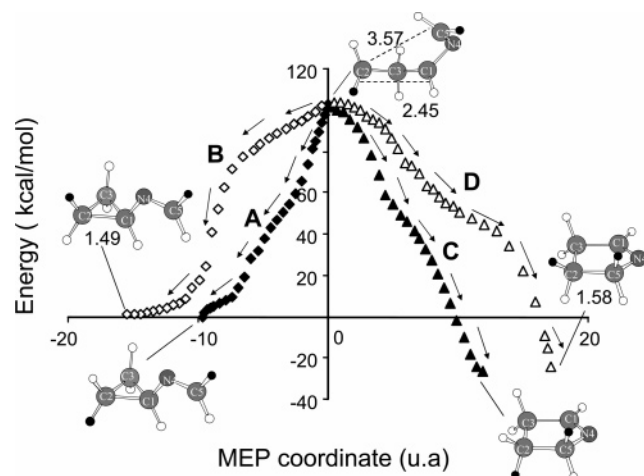


Figure 6. Energy profiles along the four S_0 MEPs connecting the S_0/S_1 CI point to the photoproducts for model compound **3**. Path A leads to reactant back-formation. Path B leads to cyclopropane isomerization. Paths C and D lead to two stereoisomeric pyrrolines. Marked hydrogens illustrate the stereochemistry. Geometrical parameters are shown in Å and degrees.

diradicals. These two species have high energies in S_0 and therefore no relaxation paths will lead from the CI_{S_1/S_0} to these two compounds. Consequently, only \mathbf{x}_1 and \mathbf{x}_2 represent significant relaxation paths from the CI_{S_1/S_0} region.

For model **3**, four different direct relaxation paths have been located leading to four possible products. This means that, potentially, all four products can be considered primary photoproducts and can originate by a single decay channel. Two of these channels (paths A and B in Figure 6) connect the CI_{S_1/S_0} to the initial cyclopropylimine through two paths that differ in the direction of rotation about the $\text{C}_2\text{—C}_3$ single bond. These paths are stereochemically distinct as, for a labeled compound, they would lead to back-formation of the original reactant (path A) or to formation of a reactant stereoisomer characterized by *cis/trans* ring isomerization (path B). Indeed, one path describes the reactant back-formation due to the interaction of the unpaired electrons located on the imine moiety and the methylene group. As an alternative, the second path describes a situation where the terminal methylene can rotate along the $\text{C}_2\text{—C}_3$ bond before the decay occurs. Once this rotation has started, the reactant back-formation process is prevented because of the absence of an interaction between the corresponding orbitals. The decay and closure could take place after a 180° rotation to yield a new cyclopropane where ring isomerization has occurred.

The other two paths (paths C and D in Figure 6) connect the CI_{S_1/S_0} to the pyrroline. In a similar way to the cyclopropylimine path, we find that a different direction of rotation about $\text{C}_2\text{—C}_3$ bond leads to the formation of two different, isomeric pyrrolines. In **3**, the final pyrroline is again the same for both paths, but with a stereochemically labeled derivative the two paths would be distinct. This situation is represented in Figure 6, where marked hydrogen atoms are used to illustrate the movements along the alternative paths. The two corresponding relaxation paths show the same features, with an initial flat region (i.e., energy profile) corresponding to a coordinate where C_2 and C_5 must approach one another sufficiently closely to allow orbital interaction, as described above. The need for this interaction makes back-formation of the cyclopropane ring easier and energetically favorable along this plateau when the shifting C_2 methylene does not rotate (note the larger initial slopes of path A and path B with respect to those of paths C and D). As a consequence, the molecules traveling along the initial flat region will hardly reach the path leading to pyrroline formation but are more likely to follow one of the steepest descents leading to the reactant.

At this point notice that, in principle, our computations suggest that all types of pyrroline stereochemistry (*sr*, *si*, *ar*, and *ai*) are possible through a combination of the S_1 and S_0 branches of the photochemical reaction path. In particular, the suprafacial/antarafacial selection is determined by the preferential direction of rotation about the $\text{N}_4\text{—C}_5$ bond. On the other hand, the inversion/retention preference seems to be determined immediately after the decay during the initial S_0 relaxation by the factors that determine the preferentially populated relaxation path.

The analysis of our results supports a qualitative agreement between the experimentally and computationally derived mechanistic pictures. First, the low quantum yields observed for the rearrangement reaction are due to the higher probability of reactant back-formation after ground-state decay (i.e., because of the higher slope of path A, only a small fraction of the molecules reaching the CI_{S_1/S_0} may follow a path leading to the rearranged photoproducts). Second, the observed reaction stereochemistry is consistent with the calculated paths. In fact, when the single bond between C_2 and C_3 does not rotate, both radicals in C_2 and C_5 can interact, after a small conformational change, to give the pyrroline with the observed stereochemistry (see Figure 6, path C). However, rotation of the terminal methylene in C_2 would force the molecule to follow a ridge along the PES with almost no energy decrease, changing its geometry until it could finally enter the relaxation channel leading to the pyrroline with the opposite stereochemistry (see Figure 6, path D). The competition between decay and methylene rotation is also consistent with the experimental fact that the *trans*-cyclopropylimines yield mainly the *trans*-pyrrolines, while the *cis*-cyclopropylimines mainly yield the *cis*-pyrrolines.

The geometry and energy of the CI_{S_1/S_0} points are predicted to be sensitive to substituents placed on the imine or cyclopropane moieties. In particular, while bulky substituents will only interact weakly in the ground-state equilibrium structures or in the CI structure derived from *trans*-cyclopropylimines, they will interact more strongly at CI_{S_1/S_0} related to *cis*-cyclopropylimines. Accordingly, to avoid steric repulsion, the terminal methylene rotates and thus prompts the isomerization to the *trans*-isomer.

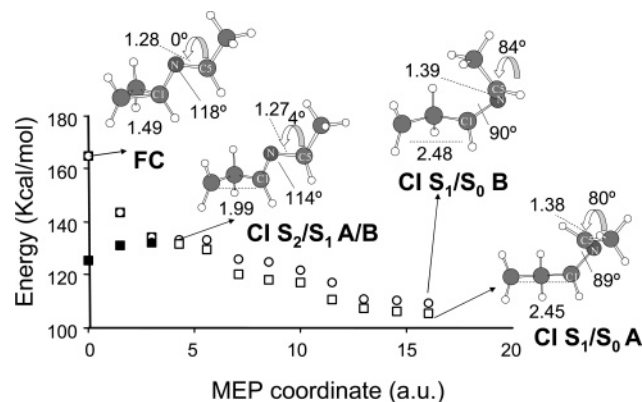


Figure 7. Energy profiles along the MEP for the two paths describing the relaxation from the FC point to the ground state for model compound **4**. Geometrical parameters are shown in Å and degrees.

The consequences of this effect can be observed in the measured quantum yield of **1f**, where *cis*-to-*trans* isomerization was more efficient than the reverse process, and in the monitoring experiment on **1e**, where *cis*-**1e** was not observed at all (see Section 2.2).

3.4. Methyl Derivatives. As explained above, the suprafacial or antarafacial stereochemical outcome is entirely determined in the excited state (where clockwise and counterclockwise rotation about the N4–C5 bond is determined). Only one product can be generated when indistinguishable substituents are present on the iminic carbon (see Table 1). However, when the substituents are different, as in *trans*-**1e**, two products may be generated. This situation has been observed experimentally for the thermal version of the vinylcyclopropane–cyclopentene rearrangement, where the preference for the *si* versus *ai* stereochemistry in the *trans*-cyclopropane is higher as the steric difference between the two vinylic substituents becomes more marked.⁷ To explain the experimental findings outlined above for the photochemical reaction, we calculated two different excited-state paths for the methylated derivative **4**. The results are shown in Figure 7.

Two different paths that end in two different conical intersections (CI_{S₁/S₀A and CI_{S₁/S₀B) differing in the sense of rotation about the N₄–C₅ bond were found. It can be seen that these paths coincide on S₂ since the reaction coordinate is dominated by the common cyclopropane bond-breaking step. However, on S₁ the torsional deformation moves one of the substituents closer to C₂ and the different steric hindrance of the two iminic substituents causes a slight, but clear, energy difference between the paths. Comparing these two paths, the lower in energy is a given path, the wider is the energy valley defined by that path. As a consequence, a wider valley is expected to collect more ground-state trajectories (starting at the S₁/S₀ conical intersection) thus indicating the dominant stereoisomer. In this model, the path with the steepest descent will be preferred and the greater the energy difference between the two substituents, the greater the preference for one of the two possible paths. This is in agreement with the experimental findings for imines **1d** (R³ = H, R⁴ = Ph, 10:1 mixture) and **1e** (R³ = Me, R⁴ = Ph, 3:1 mixture). This situation causes the molecule to decay to the ground state with the suprafacial or antarafacial stereochemistry already determined. The ratio between the suprafacial and antarafacial products is therefore guided by the relative energies of the paths connecting the FC region with the CI_{S₁/S₀ A and B.}}}

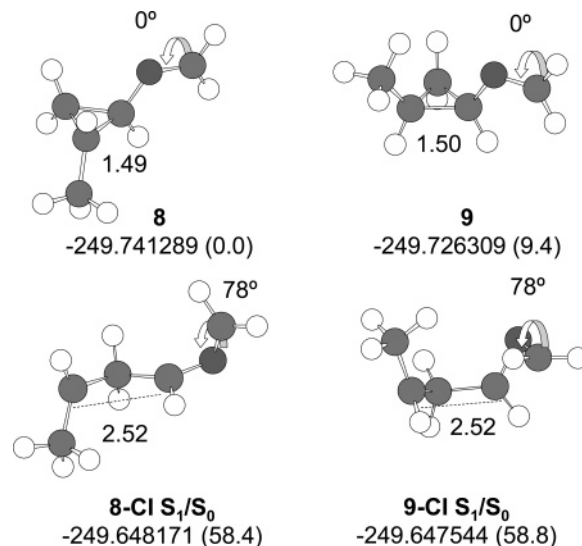


Figure 8. FC and CI geometries (parameters in Å and degrees) and energies (in brackets, values relative to the ground-state minimum of **8**) for model compounds **8** and **9**.

However, the inclusion of dynamic factors at this point would be necessary to completely establish the origin of the observed ratios. Once reaching one of these CI_{S₁/S₀'s, the ground-state decay causes the molecule to follow one of the four reaction paths discussed above that appear to control the inversion/retention of stereochemistry at C₂. Thus, for substituted imines, eight different paths are available through two different diastereomeric conical intersections.}

Combination of the results obtained for **3** and **4** allows for a rationalization of the observed product distribution (see Figures 1 and 2). In the cases where the iminic substituents are sufficiently different (such as in **1d**), the lower energy excited state path will mainly select one of the two possible CI_{S₁/S₀'s. Of course, ground-state relaxation will lead to the production of the corresponding final pyrroline. The combination of the selected S₁ and S₀ paths lead to preferential production of only one of the **2d** stereoisomers. However, when the two iminic substituents have similar sizes (such as in **1e**), the two diastereoselective S₁ paths must have similar energies and photoexcitation will yield products with either suprafacial or antarafacial stereochemistry (i.e., *trans*-**2e** and *cis*-**2e**). However, it is important to stress that although the MEPs qualitatively rationalize the stereochemistry of the detected products, dynamical effects may influence the exact product distribution and the stereochemical scrambling.}

While the substitution on the iminic carbon greatly affects the product distribution, substitution on C₂ seems to mainly affect the regiochemistry of the reaction and the ratio between ring isomerization and rearrangement.^{3,4,6,7} This observation can be explained by the fact that the absence of a real diradical intermediate in the excited state does not allow equilibration and, therefore, the original conformation is maintained until the S₁→S₀ decay. To assess the effect of substitution at C₂, we calculated the relevant stationary points for the methyl derivatives **8** and **9** (Figure 8). It can be seen how the S₁/S₀ conical intersections present similar geometries and energies. This is consistent with the small influence that C₂ substitution has on the reaction. However, a difference of 9 kcal/mol in the S₀ energies of the *cis* (compound **9**) and *trans* (compound **8**)

Table 2. CASPT2/6-31G* Relative Energies Calculated for *N*-Cyclopropylimines

structure	state	relative CASPT2 energy (kcal mol ⁻¹)	structure	state	relative CASPT2 energy (kcal mol ⁻¹)
1a-FC ^c	S ₂	125.5	5-FC ^c	S ₂	180.5
	S ₁	96.2		S ₁	110.3
	S ₀	0.0 ^a		S ₀	0.0 ^a
3-FC ^c	S ₂	170.2	6-FC ^c	S ₂	152.6
	S ₁	122.8		S ₁	108.3
	S ₀	0.0 ^a		S ₀	0.0 ^a
3-CI _{S₂/S₁}	S ₂	127.3	7-FC ^c	S ₂	153.1
	S ₁	127.3		S ₁	113.6
	S ₀	113.3		S ₀	0.0 ^a
3-CI _{S₁/S₀}	S ₂	166.1	8-FC ^c	S ₂	159.2
	S ₁	115.0		S ₁	102.6
	S ₀	110.4		S ₀	0.0 ^a
pyrroline ^c	S ₀	-26.2	8-CI _{S₁/S₀}	S ₂	137.6
4-FC ^c	S ₂	164.9		S ₁	61.5
	S ₁	125.4		S ₀	58.4
	S ₀	0.0 ^a	9-FC ^c	S ₂	164.3 ^b
4-CI _{S₂/S₁} -A	S ₂	135.1		S ₁	95.3 ^b
	S ₁	132.0		S ₀	9.4 ^b
	S ₀	35.3	9-CI _{S₁/S₀}	S ₂	132.6 ^b
4-CI _{S₂/S₁} -B	S ₂	135.0		S ₁	61.0 ^b
	S ₁	134.4		S ₀	58.8 ^b
	S ₀	37.6			
4-CI _{S₁/S₀} -A	S ₂	168.5			
	S ₁	84.9			
	S ₀	82.0			
4-CI _{S₁/S₀} -B	S ₂	148.0			
	S ₁	109.2			
	S ₀	108.9			

^a For each compound, the energy values are relative to the ground-state energy of the cyclopropane. ^b Energy relative to the ground state of cyclopropane **8**. ^c Geometry optimized with single-root CASSCF wave function.

isomers (see Table 2) exists in the ground state, and this could affect the ring isomerization. In fact, it was experimentally observed (i.e., monitoring the rearrangement of **1d**) that the cis isomer isomerizes slightly faster than the trans isomer. In the presence of a greater steric effect, such as in **1e** and **1f**, the

trans formation from the cis isomer is so fast that the less stable cis isomer could not be detected at all by ¹H NMR spectroscopy.

4. Conclusions

The study described above shows that a combined computational and experimental investigation of the photorearrangement of *N*-cyclopropylimines to pyrrolines yields a mechanism that is consistent with the observed product distribution, regiochemistry, and stereochemistry of the reaction. Light absorption promotes the molecule to S₂, which corresponds to the singlet $\pi-\pi^*$ spectroscopic state. The subsequent relaxation to the ground state is driven by a path dominated by cyclopropane σ -bond breaking in S₂, rotation of the iminic moiety in S₁, and photoproduct formation in S₀. The stereochemistry observed for the iminic moiety is explained in terms of the change in relative stabilities of the paths describing the formation and decay of a nonequilibrated (transient) diradical when the iminic substituents are changed. The absence of an equilibrated excited-state intermediate along the reaction path is consistent with the lack of solvent effects, side reactions, or measurable fluorescence. Quantum yield measurements and product studies show that, in agreement with the computed reaction mechanism, the ring isomerization and the rearrangement have similar rates.

Acknowledgment. We thank the Spanish MCyT (BQU2001-1625), the Universidad de La Rioja (API-02/B08), and the Comunidad Autónoma de La Rioja (ACPI-2003/08) for financial support. A.S. and D.S. thank the Spanish MECyD for their grants.

Supporting Information Available: Complete experimental procedures, characterization data for new compounds, and Cartesian coordinates and absolute energies for the geometries discussed in the text. This material is available free of charge via the Internet at <http://pubs.acs.org>.

JA0467566